Giant Room-Temperature Magnetocaloric Effect Across the Magnetostructural Transition in $(MnNiSi)_{1-x}(FeCoGa)_x$ Alloys

Subrata Ghosh[1,*], Arup Ghosh[2], Pintu Sen[3] and Kalyan Mandal[1]

[1]*Magnetism Laboratory, Department of Condensed Matter Physics and Material Sciences, S. N. Bose National Centre for Basic Sciences, Block-JD, Sector-III, Salt Lake, Kolkata 700106, India*

[2]*Condensed Matter Physics Division, Saha Institute of Nuclear Physics, 1/AF Bidhannagar, Kolkata 700 064, India*

[3]*Physics Group, Variable Energy Cyclotron Centre, 1/AF Bidhannagar, Kolkata 700064, India*

Magnetic and structural transitions are observed to coincide at around room temperature in transition-metal-based $(MnNiSi)_{1-x}(FeCoGa)_x$ ($x = 0.15$ and 0.16) alloys, which leads to a coupled first-order magnetostructural transition (MST) from paramagnetic hexagonal to ferromagnetic orthorhombic structure, and, as a result, a giant magnetocaloric effect is observed in these alloys. With subsequent doping for $x = 0.17$, the MST decouples into two separate transitions, structural and magnetic, although the transitions couple upon enhancing the applied magnetic field. The alloys with $x = 0.15$, 0.16, and 0.17 are found to exhibit isothermal magnetic entropy changes ($|\Delta S_M|$) as large as about $25 \, \mathrm{J \, kg^{-1} \, K^{-1}}$ at 323 K, about $31.1 \, \mathrm{J \, kg^{-1} \, K^{-1}}$ at 281 K, and about $23.8 \, \mathrm{J \, kg^{-1} \, K^{-1}}$ at 213 K, respectively, due to a field change of $\Delta H = 50$ kOe. These low-cost materials may be considered as promising candidates for magnetic refrigeration around room temperature due to their giant magnetocaloric properties, with significantly large relative cooling power (RCP = 191.8, 209.6, and 139.2 J/kg, respectively, for $x = 0.15$, 0.16, and 0.17 due to $\Delta H = 50$ kOe).

I. INTRODUCTION

Energy-efficient and eco-friendly magnetic refrigeration (MR) technology based on the magnetocaloric effect (MCE), which has enormous potential to replace conventional vapor compression technology, is expected to be applicable in solid-state-based modern refrigeration devices [1,2]. In this regard, it requires potential refrigerant materials with giant magnetocaloric properties. Materials such as $Gd_5Si_2Ge_2$ [3], $La(Fe, Si)_{13}$-based alloys [4–6], Mn-Fe-based compounds [6,7], and Ni-Mn-based Heusler alloys [8–12] are being already proposed as promising refrigerant materials because of their excellent MCEs around room temperature. All of these alloys are accompanied with a magnetic-field-induced structural transition from an antiferromagnetic or paramagnetic (PM) phase to a ferromagnetic (FM) phase, leading to a strongly coupled magnetostructural transition (MST), which is associated with significant changes in unit-cell volume, and therefore, a sharp change in magnetization across the phase transition. However, it is a great challenge to discover such giant magnetocaloric materials with transition-metal-based less-expensive earth-abundant nontoxic elements.

Intermetallic compounds with the general formula MnTX (T = Ni, Co and X = Si, Ge) have recently attracted considerable attention because of their potential to show interesting multifunctional properties, such as MSTs, a magnetic shape memory effect, a large MCE, giant magnetoresistance, and volume anomalies [13–17]. All abovementioned stoichiometric materials exhibit a second-order magnetic transition followed by a first-order structural transformation from low-temperature orthorhombic to a high-temperature hexagonal structure in the paramagnetic region, with no significant changes in magnetization. Magnetoresponsive properties, such as MCE and magnetoresistance, are associated solely with changes in magnetization. Therefore, shifting of the structural transition of these materials to the ferromagnetic region or coupling it with a magnetic transition near room temperature may be the best option to enrich them with the abovementioned properties. To obtain a MST for these compounds, several effective methods, such as elemental substitution, off-stoichiometry, isostructural substitution, heat treatment, or application of external parameter like hydrostatic pressure, are introduced [14,18–22]. MnNiGe- and MnCoGe-based systems have closeness between their magnetic and structural transitions, and thus, are extensively studied to achieve MSTs using the abovementioned techniques.

*subrataghosh728@bose.res.in

Stoichiometric MnNiGe [23] shows a magnetic transition at a Neel temperature (T_N) of about 346 K and a structural transition at $T_M \sim 470$ K, whereas MnCoGe [24] shows a magnetic transition at the Curie temperature (T_C) of about 355 K and structural transitions at $T_M \sim 372$ K.

In addition to the abovementioned systems, the ferromagnetic MnNiSi [25] system also exhibits a second-order FM to PM transition at $T_C \sim 622$ K and, beyond that temperature, a structural transformation from TiNiSi-type orthorhombic to Ni$_2$In-type hexagonal structure at a higher temperature of about $T_M \sim 1210$ K. Hence, it is difficult to obtain a MST at room temperature for this compound. However, considering the relatively low cost of the raw materials, it will be commercially viable to use them for domestic purposes. In this present work, it is observed that, by alloying the MnNiSi system with that of FeCoGa, a hexagonal structure is stabilized near room temperature from 1210 K, and, for a nominal composition of (MnNiSi)$_{1-x}$(FeCoGa)$_x$ ($x = 0.15$ and 0.16), a MST is achieved at around room temperature. Substitution of Fe, with relative lower atomic radius, in place of Mn increases orthorhombic distortion and stabilizes the hexagonal phase at lower temperature, resulting in a reduction of both T_C and T_M towards room temperature with lower saturation magnetization [17]. To compensate for the reduction in magnetization, Co can be doped in place of Ni, where Co enhances the ferromagnetic interaction to the system. Ga, with a much larger atomic radius than that of Si, again enhances faster orthorhombic distortion to the system, which couples T_C and T_M, and, as a result, a MST is obtained in the vicinity of room temperature.

II. EXPERIMENTAL DETAILS

Polycrystalline (MnNiSi)$_{1-x}$(FeCoGa)$_x$ ($x = 0.15, 0.16,$ and 0.17) samples are prepared by a conventional arc melting technique under 99.99% purity of argon atmosphere using appropriate amounts of high-purity constituent elements from Sigma Aldrich. An additional amount of 3% Mn is taken to compensate for its weight loss during melting. The samples are turned and remelted several times (7 to 8 times) to maintain the compositional homogeneity. All as-prepared samples are sealed in an evacuated quartz tube and annealed at 1173 K for four days, followed by quenching in ice water. X-ray diffraction patterns of all samples are obtained using a PANalytical X'pert PRO diffractometer with Cu $K\alpha$ radiation. Magnetic measurements are performed using a SQUID vibrating sample magnetometer (MPMS, Quantum Design) with a maximum applied magnetic field of 50 kOe.

III. RESULTS AND DISCUSSION

Figure 1 depicts the x-ray diffraction patterns at room temperature ($\sim$300 K) for all investigated alloys. On enhancing the doping amount of (FeCoGa)$_x$ in
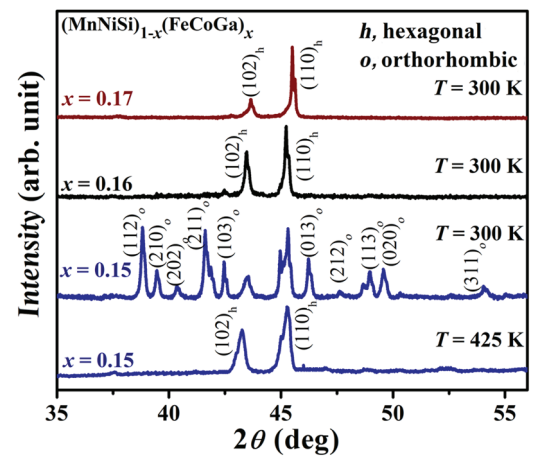

FIG. 1. X-ray diffraction patterns for (MnNiSi)$_{1-x}$(FeCoGa)$_x$ ($x = 0.15, 0.16,$ and 0.17) alloys at 300 K, and x-ray diffraction pattern for $x = 0.15$ alloy at 425 K. Here, o and h represent orthorhombic and hexagonal phases, respectively.

(MnNiSi)$_{1-x}$, from $x = 0.15$ to 0.17, a structural phase transformation from orthorhombic to hexagonal is observed, which indicates shifting of the structural transition towards room temperature from the structural transition temperature of the parent MnNiSi alloy at about 1210 K. An orthorhombic phase with some traces of hexagonal phase is observed for the $x = 0.15$ alloy, whereas $x = 0.16$ is found to show a dominating hexagonal phase and $x = 0.17$ displays a pure hexagonal phase. The unit-cell lattice parameters in the orthorhombic phase for the alloy with $x = 0.15$ are found to be $a_o = 5.835$ Å, $b_o = 3.71$ Å, and $c_o = 6.905$ Å, whereas for $x = 0.17$ in the hexagonal phase the parameters are $a_h = 3.982$ Å and $c_h = 5.179$ Å. From a crystallographic study [23], the orthorhombic unit cell is related to the hexagonal unit cell through the following relations:, $a_o = c_h$, $b_o = a_h$, and $c_o = \sqrt{3}a_h$. Here, the decrease in the c_h/a_h (or a_o/b_o) ratio from 1.573 for $x = 0.15$ to 1.301 for $x = 0.17$ can distort the geometry of the orthorhombic structure and makes the hexagonal structure more stable at lower temperature [26], resulting in a decrease in the structural transition temperature with increasing x. A further x-ray diffraction pattern is recorded at 425 K for the alloy with $x = 0.15$, and it is found to exhibit only the hexagonal phase. A large change in unit-cell volume of about -3.18% is observed across the structural transformation from a high-temperature hexagonal phase to a low-temperature orthorhombic phase.

The temperature dependence of the zero-field cooled (ZFC) and field-cooled (FC) magnetization (M-T curves) within 100–400 K in the presence of 500 Oe magnetic field for (MnNiSi)$_{1-x}$(FeCoGa)$_x$ ($x = 0.15, 0.16,$ and 0.17) alloys are shown in Fig. 2. On increasing the doping amount from $x = 0.15$ to 0.16, the magnetostructural transition temperature (T_t), estimated from the plot of
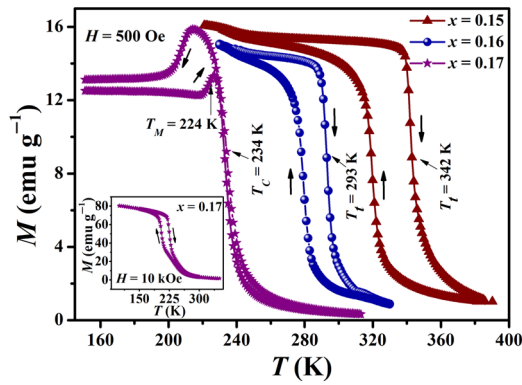
FIG. 2. *M-T* curves for (MnNiSi)$_{1-x}$(FeCoGa)$_x$ ($x = 0.15$, 0.16, and 0.17) alloys in the presence of 500 Oe magnetic field. (Inset: *M-T* curve for the alloy with $x = 0.17$ in the presence of 10 kOe field).

FIG. 3. Isothermal *M-H* curves during heating mode in the temperature regime of 280–304 K for the alloy with $x = 0.16$.

$dM/dT - T$ in the heating cycle, is found to shift from about 342 K to a lower temperature of about 293 K. The presence of a thermal hysteresis between heating and cooling cycles in the *M-T* curve clearly signifies the coincidence of both the magnetic transition from FM to PM and a structural transition from low-temperature orthorhombic to high-temperature hexagonal at the same temperature, which leads to a first-order transition. On further enhancement of the doping amount to $x = 0.17$, the MST decouples and, as a result, separate structural transformations in the ferromagnetic region and magnetic transition are observed at $T_M = 224$ K and $T_C = 234$ K, respectively. However, the separated structural and magnetic transitions are found
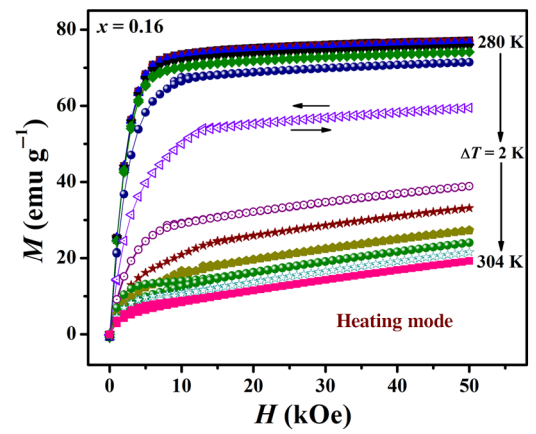
to coincide upon enhancing the magnetic field, which is shown in the inset of Fig. 2. The width of the thermal hysteresis between ZFC and FC curves during the MST are found to be 23 and 14 K for the alloys with $x = 0.15$ and 0.16, respectively. Therefore, the thermal hysteresis decreases significantly with an increase in doping amount, and it is minimum for $x = 0.16$, which makes this alloy suitable for application in room-temperature magnetic refrigeration. Moreover, T_t for this investigated compound, (MnNiSi)$_{1-x}$(FeCoGa)$_x$, is tunable from 224 to 342 K with a broad temperature window of 118 K, which will be beneficial for magnetic refrigeration associated with a wide and controllable operating temperature.
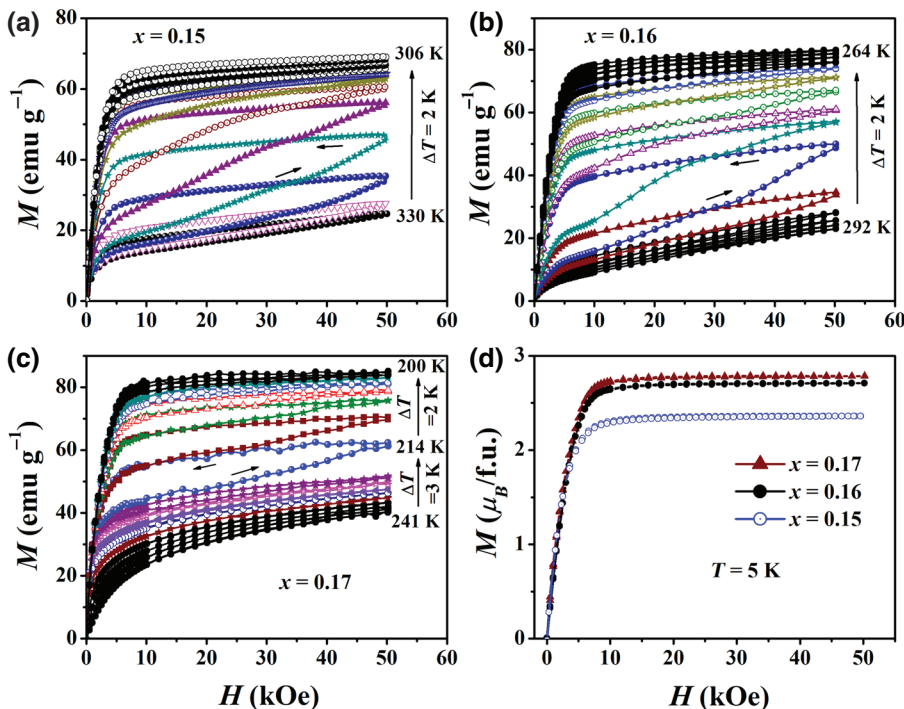

FIG. 4. Isothermal *M-H* curves at a minimum temperature interval (ΔT) of 2 K in cooling mode (PM to FM phase) for the alloys with (a) $x = 0.15$ (b) $x = 0.16$, and (c) $x = 0.17$. (d) Field dependence of magnetization (M vs H) at 5 K for all investigated alloys.
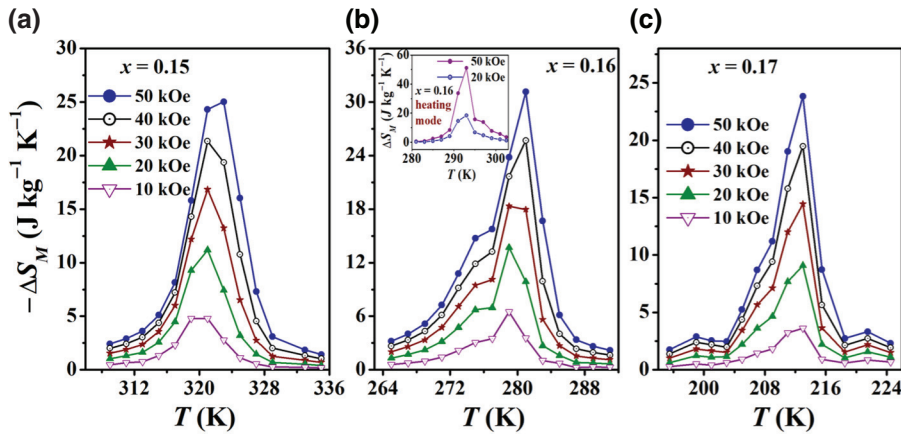
FIG. 5. Magnetic entropy change (ΔS_M) as a function of temperature due to different field variations for the alloys with (a) $x = 0.15$, (b) $x = 0.16$ [inset: estimated ΔS_M for $x = 0.16$ in heating mode due to a field change of 20 and 50 kOe], and (c) $x = 0.17$ in cooling and field increasing modes.

Isothermal field-dependent magnetization (*M-H*) curves are measured across T_t in heating mode for the sample with $x = 0.16$, up to a maximum field of 50 kOe, and are shown in Fig. 3. The heating mode is not associated with any field-induced metamagnetic transition (FIMMT); as a result, no first-order transition takes place from ferromagnetic to paramagnetic phases and it is unusual according to the results obtained from the *M-T* curves. Here, the change of 50 kOe magnetic field is not sufficient to induce a FIMMT for these alloys in heating. Therefore, isothermal *M-H* curves are measured during cooling mode for all samples from PM hexagonal phase to FM orthorhombic phase (Fig. 4). To remove the field history effect of the samples, the loop process methods are followed to measure the isotherms [27]. Figure 4 clearly shows the observation of a FIMMT in the vicinity of the magnetostructural transition temperature, which also confirms the first-order nature of the MST. The low-temperature *M-H* measurement, as shown in Fig. 4(d), is performed at 5 K for all alloys and shows a typical ferromagnetic ordering. The saturation magnetization (M_S) for the alloy with $x = 0.17$ due to a field change of 50 kOe is found to be about 104.5 emu/g (or ~ 2.79 μ_B/f.u.), which is larger than that of its parent alloy, MnNiSi [25] (~ 2.62 μ_B/f.u.)

The isothermal magnetic entropy change (ΔS_M), an essential parameter of the magnetocaloric effect, can be estimated using the Maxwell equation [1], $\Delta S_M(T, \Delta H) = \mu_0 \int_0^H \left(\frac{\partial M(H,T)}{\partial T} \right)_H dH$, from the isothermal *M-H* curves measured at discrete stable temperatures in the vicinity of their respective MSTs during the cooling mode. The ΔS_M value, as calculated using the above equation, is plotted as a function of temperature for all investigated alloys in Fig. 5 for a magnetic field change of 10–50 kOe. The estimated peaks of $|\Delta S_M|$ are found to be as large as about 25 J kg^{-1} K^{-1} at 323 K, about 31.1 J kg^{-1} K^{-1} at 281 K, and about 23.8 J kg^{-1} K^{-1} at 213 K for the alloys with $x = 0.15$, 0.16, and 0.17, respectively, due to $\Delta H = 50$ kOe, which are associated with the first-order MST. The significant jump in magnetization

across the MST arises from changes to the lattice and magnetic structure in the coupled transition, developing a giant magnetic entropy change in these investigated alloys. Moreover, $|\Delta S_M|$ for the alloy with $x = 0.16$ is calculated in heating mode, and the estimated value is observed to be 51.2 J kg^{-1} K^{-1} [shown in the inset of Fig. 5(b)], which is much higher than that of the value obtained during cooling mode. During *M-H* measurements in cooling mode, a field-induced paramagnetic to ferromagnetic transition takes place due to the application of the 50 kOe magnetic field in the vicinity of the MST. However, no such field-induced ferromagnetic to paramagnetic transition takes place during heating and the samples remains either in ferromagnetic-paramagnetic or

TABLE I. Comparison of peak values of isothermal magnetic entropy change (ΔS_M^{peak}) due to $\Delta H = 50$ kOe and the temperature where ΔS_M is maximum (T_{peak}) of (MnNiSi)$_{1-x}$(FeCoGa)$_x$ ($x = 0.15$–0.17) alloys with other promising refrigerant materials.

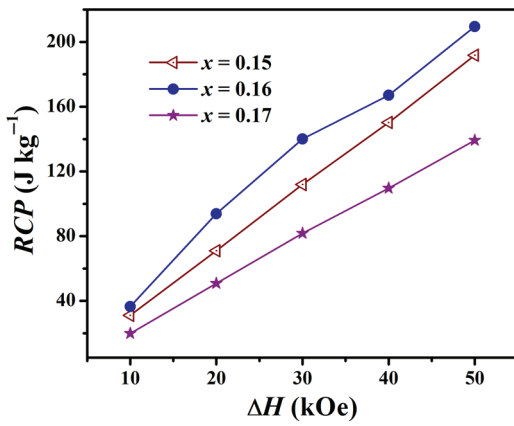| Materials	$|\Delta S_M^{peak}|$ (J kg^{-1} K^{-1})	T_{peak} (K)	Refs.
Gd	~ 10.2	294	[28]
Gd$_5$Ge$_2$Si$_2$	~ 18.5	278	[3]
La(Fe$_{0.89}$Si$_{0.11}$)$_{13}$H$_{1.3}$	~ 28.0	291	[4]
MnFeP$_{0.45}$As$_{0.55}$	~ 18	308	[29]
Ni$_{40}$Co$_{10}$Mn$_{40}$Sn$_{10}$	~ 14.9	288	[30]
Mn$_{46}$Ni$_{39.5}$Sn$_{10}$Si$_{4.5}$	~ 20.0	205	[31]
Ni$_{45}$Co$_5$Mn$_{38}$Sb$_{12}$	~ 34.0	262	[32]
Ni$_{50}$Mn$_{37}$Sn$_{13}$	~ 18.0	299	[8]
Ni$_{55.2}$Mn$_{18.6}$Ga$_{26.2}$	~ 20.4	317	[33]
MnNi$_{0.77}$Fe$_{0.23}$Ge	~ 19.0	267	[16]
Mn$_{0.82}$Fe$_{0.18}$NiGe	~ 31.0	205	
Mn$_{0.6}$Fe$_{0.4}$NiSi$_{0.93}$Al$_{0.07}$	~ 20.6	255	[22]
Mn$_{0.89}$Cr$_{0.11}$CoGe	~ 27.7	292	[34]
(MnNiSi)$_{1-x}$(FeCoGa)$_x$			Present Work
$x = 0.15$	~ 25.0	323	
$x = 0.16$	~ 31.1	281	
$x = 0.17$	~ 23.8	213	

FIG. 6. Relative cooling power (*RCP*) as a function of magnetic field change for $x = 0.15$, 0.16, and 0.17 alloys.

in the mixed phase throughout the isothermal *M-H* measurements, and, as a result, the temperature evolution of the ferromagnetic phase might lead to overestimation of the magnetic entropy change during heating. Therefore, cooling mode is preferable to calculate an accurate magnetic entropy change value for these similar materials. The peak values of ΔS_M of the investigated samples are compared with other promising refrigerant materials in Table I. These transition-based materials shows excellent magnetocaloric effects in a broad and tunable temperature region, with a minimum peak value of $|\Delta S_M|$ of 23.8 J kg^{-1} K^{-1} at 213 K due to $\Delta H = 50$ kOe.

Apart from the large magnetic entropy change, the relative cooling power (RCP) is an important parameter that defines the cooling efficiency of a magnetic refrigerant material. RCP values of these investigated alloys are estimated from the following equation: RCP = $|\Delta S_M^{\text{peak}}|\Delta T_{\text{FWHM}}$, where ΔS_M^{peak} is the peak of ΔS_M of a $\Delta S_M - T$ curve and ΔT_{FWHM} stands for the temperature range of the full width at half maximum of ΔS_M (Fig. 5). The estimated *RCP*s are plotted versus the magnetic field change in Fig. 6, and the maximum RCPs due to a field change of 50 kOe are found to be 191.8, 209.6, and 139.2 J/kg for the alloys with $x = 0.15$, 0.16, and 0.17, respectively.

From an application point of view, the refrigerant material composed of transition-metal-based, low-cost, and earth-abundant elements will be commercially cost-effective. In comparison with Mn*TX*-based intermetallic compounds, such as MnNiGe- [14,16], MnCoGe- [15,20], and other MnNiSi-based [18,19,21] systems, which also exhibit a first-order MST near room temperature, our investigated system, $(\text{MnNiSi})_{1-x}(\text{FeCoGa})_x$, is Ge free and contains a very low doping amount of Ga, resulting in the materials being very cheap. Thus, the present system made of low-cost abundant materials with large M_S, a tunable MST, a giant magnetocaloric effect, and a

large RCP will be highly attractive for implementation in room-temperature magnetic refrigeration technology.

IV. CONCLUSION

The magnetostructural phase transition from paramagnetic hexagonal to a ferromagnetic orthorhombic structure within a well-regulated broad temperature region of 224–342 K surrounding room temperature, along with tunable giant magnetocaloric properties, are observed in $(\text{MnNiSi})_{1-x}(\text{FeCoGa})_x$ ($x = 0.15$–0.17) alloys. The alloys with $x = 0.15$, 0.16, and 0.17 show significantly large $|\Delta S_M|$ values of about 25, 31.1, and 23.8 J kg^{-1} K^{-1}, respectively, for the field change of $\Delta H = 50$ kOe. Here, $x = 0.17$ is the maximal doping content to keep the magnetostructural transition coupled for this system, as a higher doping level splits it into two separate transitions. Moreover, cooling mode is found to be preferred to estimate the precise magnetic entropy change for this type of material. The investigated compound, $(\text{MnNiSi})_{1-x}(\text{FeCoGa})_x$, is a very promising refrigerant material for room-temperature nature-friendly magnetic refrigeration technology because of its tunable giant magnetocaloric properties around room temperature associated with a large relative cooling power.

[1] K. A. Gschneidner, Jr., V. K. Pecharsky, and A. O. Tsokol, Recent developments in magnetocaloric materials, Reports Prog. Phys. **68**, 1479 (2005).

[2] L. Mañosa and A. Planes, Materials with giant mechanocaloric effects: Cooling by strength, Adv. Mater. **29**, 1603607 (2017).

[3] V. K. Pecharsky and K. A. Gschneidner, Jr., Giant Magnetocaloric Effect in Gd$_5$(Si$_2$Ge$_2$), Phys. Rev. Lett. **78**, 4494 (1997).

[4] A. Fujita, S. Fujieda, Y. Hasegawa, and K. Fukamichi, Itinerant-electron metamagnetic transition and large magnetocaloric effects in La(Fe$_x$Si$_{1-x}$)$_{13}$ compounds and their hydrides, Phys. Rev. B **67**, 104416 (2003).

[5] J. Liu, J. D. Moore, K. P. Skokov, M. Krautz, K. Löwe, A. Barcza, M. Katter, and O. Gutfleisch, Exploring La(Fe, Si)$_{13}$-based magnetic refrigerants towards application, Scr. Mater. **67**, 584 (2012).

[6] O. Gutfleisch, T. Gottschall, M. Fries, D. Benke, I. Radulov, K. P. Skokov, H. Wende, M. Gruner, M. Acet, P. Entel, and

M. Farle, Mastering hysteresis in magnetocaloric materials, Philos. Trans. R. Soc. A **374**, 20150308 (2016).

[7] H. Wada and Y. Tanabe, Giant magnetocaloric effect of $MnAs_{1-x}Sb_x$, Appl. Phys. Lett. **79**, 3302 (2001).

[8] T. Krenke, E. Duman, M. Acet, E. F. Wassermann, X. Moya, L. Mañosa, and A. Planes, Inverse magnetocaloric effect in ferromagnetic Ni–Mn–Sn alloys, Nat. Mater. **4**, 450 (2005).

[9] R. Kainuma, Y. Imano, W. Ito, Y. Sutou, H. Morito, S. Okamoto, O. Kitakami, K. Oikawa, A. Fujita, T. Kanomata, and K. Ishida, Magnetic-field-induced shape recovery by reverse phase transformation, Nature **439**, 957 (2006).

[10] A. Ghosh and K. Mandal, Effect of Fe substitution on the magnetic and magnetocaloric properties of Mn-rich Mn-Ni-Fe-Sn off-stoichiometric heusler alloys, J. Appl. Phys. **117**, 093909 (2015).

[11] L. Huang, D. Y. Cong, L. Ma, Z. H. Nie, Z. L. Wang, H. L. Suo, Y. Ren, and Y. D. Wang, Large reversible magnetocaloric effect in a Ni-Co-Mn-In magnetic shape memory alloy, Appl. Phys. Lett. **108**, 032405 (2016).

[12] J. Liu, T. Gottschall, K. P. Skokov, J. D. Moore, and O. Gutfleisch, Giant magnetocaloric effect driven by structural transitions, Nat. Mater. **11**, 620 (2012).

[13] N. T. Trung, L. Zhang, L. Caron, K. H. J. Buschow, and E. Brück, Giant magnetocaloric effects by tailoring the phase transitions, Appl. Phys. Lett. **96**, 172504 (2010).

[14] T. Samanta, I. Dubenko, A. Quetz, S. Temple, S. Stadler, and N. Ali, Magnetostructural phase transitions and magnetocaloric effects in $MnNiGe_{1-x}Al_x$, Appl. Phys. Lett. **100**, 052404 (2012).

[15] S. C. Ma, Y. X. Zheng, H. C. Xuan, L. J. Shen, Q. Q. Cao, D. H. Wang, Z. C. Zhong, and Y. W. Du, Large roomtemperature magnetocaloric effect with negligible magnetic hysteresis losses in $Mn_{1-x}V_xCoGe$ alloys, J. Magn. Magn. Mater. **324**, 135 (2012).

[16] E. Liu, W. Wang, L. Feng, W. Zhu, G. Li, J. Chen, H. Zhang, G. Wu, C. Jiang, H. Xu, and F. de Boer, Stable magnetostructural coupling with tunable magnetoresponsive effects in hexagonal ferromagnets, Nat. Commun. **3**, 873 (2012).

[17] Y. Li, Z. Y. Wei, E. K. Liu, G. D. Liu, S. G. Wang, W. H. Wang, and G. H. Wu, Structural transitions, magnetic properties, and electronic structures of Co(Fe)-doped MnNiSi compounds, J. Appl. Phys. **117**, 17C117 (2015).

[18] J.-H. Chen, A. Us Saleheen, S. K. Karna, D. P. Young, I. Dubenko, N. Ali, and S. Stadler, Tuning martensitic transitions in $(MnNiSi)_{0.65}(Fe_2Ge)_{0.35}$ through heat treatment and hydrostatic pressure, J. Appl. Phys. **124**, 203903 (2018).

[19] T. Samanta, D. L. Lepkowski, A. U. Saleheen, A. Shankar, J. Prestigiacomo, I. Dubenko, A. Quetz, I. W. H. Oswald, G. T. McCandless, J. Y. Chan, P. W. Adams, D. P. Young, N. Ali, and S. Stadler, Hydrostatic pressure-induced modifications of structural transitions lead to large enhancements of magnetocaloric effects in MnNiSi-based systems, Phys. Rev. B **91**, 020401(R) (2015).

[20] C. L. Zhang, H. F. Shi, E. J. Ye, Y. G. Nie, Z. D. Han, and D. H. Wang, Magnetostructural transition and magnetocaloric effect in MnCoGe–NiCoGe system, J. Alloys Compd. **639**, 36 (2015).

[21] C. L. Zhang, H. F. Shi, E. J. Ye, Y. G. Nie, Z. D. Han, B. Qian, and D. H. Wang, Magnetostructural transition and magnetocaloric effect in MnNiSi-Fe_2Ge system, Appl. Phys. Lett. **107**, 212403 (2015).

[22] S. Ghosh, P. Sen, and K. Mandal, Magnetostructural transition and large magnetocaloric effect in $(Mn_{0.6}Fe_{0.4})NiSi_{1-x}Al_x$ ($x = 0.06$–0.08) alloys, J. Magn. Magn. Mater. **500**, 166345 (2020).

[23] W. Bazela, A. Szytuła, J. Todorović, Z. Tomkowicz, and A. Zięba, Crystal and magnetic structure of NiMnGe, Phys. Status Solidi **38**, 721 (1976).

[24] E. K. Liu, W. Zhu, L. Feng, J. L. Chen, W. H. Wang, G. H. Wu, H. Y. Liu, F. B. Meng, H. Z. Luo, and Y. X. Li, Vacancy-tuned paramagnetic/ferromagnetic martensitic transformation in Mn-poor $Mn_{1-x}CoGe$ alloys, EPL **91**, 17003 (2010).

[25] V. Johnson and C. G. Frederick, Magnetic and crystallographic properties of ternary manganese silicides with ordered Co2P structure, Phys. Status Solidi **20**, 331 (1973).

[26] G. A. Landrum, R. Hoffmann, J. Evers, and H. Boysen, The TiNiSi family of compounds: Structure and bonding, Inorg. Chem. **37**, 5754 (1998).

[27] L. Caron, Z. Q. Ou, T. T. Nguyen, D. T. Cam Thanh, O. Tegus, and E. Brück, On the determination of the magnetic entropy change in materials with first-order transitions, J. Magn. Magn. Mater. **321**, 3559 (2009).

[28] S. Y. Dan'kov, A. M. Tishin, V. K. Pecharsky, and K. A. Gschneidner, Magnetic phase transitions and the magnetothermal properties of gadolinium, Phys. Rev. B **57**, 3478 (1998).

[29] O. Tegus, E. Brück, K. H. J. Buschow, and F. R. de Boer, Transition-metal-based magnetic refrigerants for roomtemperature applications, Nature **415**, 150 (2002).

[30] L. Huang, D. Y. Cong, H. L. Suo, and Y. D. Wang, Giant magnetic refrigeration capacity near room temperature in $Ni_{40}Co_{10}Mn_{40}Sn_{10}$ multifunctional alloy, Appl. Phys. Lett. **104**, 132407 (2014).

[31] A. Ghosh, P. Sen, and K. Mandal, Measurement protocol dependent magnetocaloric properties in a Si-doped Mn-rich Mn-Ni-Sn-Si off-stoichiometric heusler alloy, J. Appl. Phys. **119**, 183902 (2016).

[32] A. K. Nayak, K. G. Suresh, and A. K. Nigam, Giant inverse magnetocaloric effect near room temperature in Co substituted NiMnSb heusler alloys, J. phys. D. Appl. Phys. **42**, 035009 (2009).

[33] X. Zhou, W. Li, H. P. Kunkel, and G. Williams, A criterion for enhancing the giant magnetocaloric effect: (Ni–Mn–Ga)—a promising new system for magnetic refrigeration, J. Phys. Condens. Matter **16**, L39 (2004).

[34] N. T. Trung, V. Biharie, L. Zhang, L. Caron, K. H. J. Buschow, and E. Brück, From single- to double-first-order magnetic phase transition in magnetocaloric $Mn_{1-x}Cr_xCoGe$ compounds, Appl. Phys. Lett. **96**, 162507 (2010).